Conference on Modelling Fluid Flow (CMFF'22)
The 18th International Conference on Fluid Flow Technologies
Budapest, Hungary, August 30 -September 2, 2022

ARTIFICIAL INTELLIGENT ENHANCED VIRTUAL BLADE MODEL

Gábor ZIPSZER[1], Szilárd VARRÓ[2], Bence DARÁZS[3], Mátyás GYÖNGYÖSI[4], Ákos HORVÁTH[5]

[1] Corresponding Author. eCon Engineering Kft., 4th floor, Kondorosi út 3., H-1116 Budapest, Hungary. Tel.: +36-1-279-0320, E-mail: gabor.zipszer@econengineering.com
[2] Infominero Kft. E-mail: szilard.varro@hiflylabs.com
[3] eCon Engineering Kft. E-mail: bence.darazs@econengineering.com
[4] eCon Engineering Kft. E-mail: matyas.gyongyosi@econengineering.com
[5] eCon Engineering Kft. E-mail: akos.horvath@econengineering.com

ABSTRACT

The Consortium of eCon Engineering Kft. and Infominero Kft. is developing a Virtual Blade Model (VBM) enhanced by Artificial Intelligence (AI) driven three-dimensional (3D) aerodynamic corrections to be applied in airframe-propeller interaction simulations.

The aim of the paper is to demonstrate the novel concept of improving conventional VBM capabilities regardless of propeller blade geometry or operating conditions.

A conventional VBM based on blade element theory was implemented in ANSYS Fluent via User Defined Function (UDF) carrying out the derivation of spanwise aerodynamic load distributions of the propeller blade using inviscid 2D profile data. This conventional VBM was enhanced by applying 3D aerodynamic corrections determined by a stand-alone AI algorithm linked with the Fluent UDF via Python scripts. The required training data for the AI model was derived from explicit 3D propeller blade Computational Fluid Dynamics (CFD) simulations.

The AI enhanced 3D corrected VBM (3D-VBM) shows improvements in overall propeller thrust and torque predictions compared to the baseline VBM (2D-VBM) using only two-dimensional (2D) airfoil data. Furthermore, the radial distribution of blade loading, hence the velocity and pressure profiles behind the propeller plane are in better agreement with the averaged explicit solution when the 3D-VBM is used.

Keywords: artificial intelligence, AI, virtual blade model, VBM, 3D-VBM

NOMENCLATURE

A_{cell}	[m^2]	cell area
B	[-]	number of blades
C	[m]	chord length
F	[N]	force
$\underline{F}$	[N]	force vector
$F_{Glauert}$	[-]	Prandtl-Glauert tip loss factor
L	[-]	Huber loss function
$\underline{S_U}$	[N/m^3]	volumetric momentum source term
T	[K]	temperature
V	[m/s]	flight speed
V_{cell}	[m^3]	cell volume
c	[-]	force coefficient
f	[N/m]	force distribution
n	[rpm]	propeller speed of rotation
p	[Pa]	pressure
r	[m]	radius
r_{rel}	[-]	relative radius
δr	[m]	elemental radius
v	[m/s]	absolute velocity magnitude
w	[m/s]	relative velocity magnitude
θ	[deg]	blade pitch angle
$\delta\Psi$	[deg]	elemental azimuth angle
α	[deg]	angle of attack
β	[deg]	blade element angle
γ	[deg]	blade twist
ξ	[-]	AI model function
ρ	[kg/m^3]	air density
φ	[deg]	relative velocity angle
ω	[rad/s]	speed of rotation

Subscripts and Superscripts

hub	propeller hub or spinner
l, d	lift, drag
n, i	n-th or i-th in a sequence
prop	propeller
s	static
tan	tangential
tot	total
a, n, t, r	VBM cylindrical axes: axial or normal, tangential and radial
x, y, z	global cartesian axes: x, y and z
'	corrected

1. INTRODUCTION

The necessity to analyse propeller blade aerodynamics was born with the initial attempts of powered flight. It is known that the Wright Brothers designed the propeller blades for propelling the famous Wright Flyer based on profile data set they gathered from the extensive test campaign conducted within their own wind tunnel [1].

As the science of aerodynamics and its application on aircraft development progressed, the methods for propeller performance analysis developed as well providing better understanding of propeller induced flow-field and its possible effects on flight performance and control.

Nowadays, when aircraft developers need to achieve a wide variety of technical criteria and continuous performance gain is demanded by the market, there is an increasing need to account for propeller induced flow effects even in the case of small and medium size aircraft. Being aware of the propeller induced flow field from the beginning of the design process could save significant time and cost later in the optimisation and prototyping stages. Also, it can ensure improved product performance which is sought for by many aircraft developers.

Using CFD models including explicit propeller blades comes with high costs, therefore it is unaffordable during the initial stages of product development or for detailed design optimisation [2].

The Virtual Blade Model (VBM) with the industrialised Artificial Intelligence (AI) driven 3D correction method (designated as 3D-VBM) developed by the Consortium of eCon Engineering Kft. and Infominero Kft. offers a cost-effective alternative for substituting explicit blade analyses with a 3D corrected VBM providing improved prediction capabilities compared to conventional VBM techniques.

In the following chapters the developed VBM model and the 3D correction method along with the utilised AI model will be discussed, followed by the assessment of the results derived by the explicit blade CFD, conventional and 3D-VBM models.

2. CONVENTIONAL VIRTUAL BLADE MODEL

In the past few years many papers were published discussing different methods of substituting the resource-demanding explicit modelling of propellers or helicopter rotors. The thesis of Bicsák [2] and the work of Stajuda et. al. [3] provide a summary of the papers on the topic.

The simpler methods are based on the axial or the generalised momentum theory, where the propeller is represented by a disc imparting momentum to the flow through it [4] – this disc can be called as the actuator disc and the modelling technique as the Actuator Disc Model (ADM). ADM assumes averaged and constant momentum sources over the disc area.

More detailed methods use blade element theory to derive the momentum source terms based on local flow properties, the geometrical properties of the modelled propeller blade and the lift and drag coefficients of the actual airfoil section. This model can be called as Virtual Blade Model where the source terms are derived for each computational cell or node over the entire VBM sub-domain [5].

Some VBM assumes constant propeller loading around the azimuth at a given radii and apply the same radial blade load distribution over the whole VBM domain. While an enhanced VBM calculates the azimuthal load variation as well, hence providing a better approximation of the propeller or rotor load distribution and the induced flow-field.

It must be noted that in many papers the ADM and VBM acronyms and naming conventions are mixed regardless of the theory actually applied. In this paper ADM refers to the models using axial or generalised momentum theory, while VBM refers to the models applying blade element theory.

Usually, ADM and VBM models are designed to be used in steady-state CFD problems assuming that the time-averaged transient flow induced by the passing blades of a propeller or rotor eventually results in a steady-state flow-field, which can be modelled by a steady-state ADM or VBM. There are VBM and Actuator Line Model (ALM) methods which are designed to be used in unsteady CFD problems [6, 7]. The 2D-VBM and 3D-VBM presented in this paper are valid only for steady-state problems.

2.1. Applied 2D-VBM

The baseline 2D-VBM was implemented as a UDF within ANSYS Fluent finite volume CFD solver using blade element theory and the required aerodynamic and geometric parameters of the simulated propeller and its blades in the process of source term calculation.

The VBM domain built up from hexahedral elements with one-cell thickness. The VBM domain resolution – the number of cells in radial and azimuthal direction – can be adjusted, but must be evenly distributed azimuthally. The applied resolution provided smooth variable distributions behind the disc with a low cell count. The volume mesh around the VBM domain and the interfaces can be any type supported by Fluent.

In order to account for both radial and azimuthal variation of the flow field and to enable source term derivation for each cell accordingly we followed the method described by Wahono [5] to set up the core of the VBM UDF excluding the special treatment required for helicopter rotors and any of the built-in iterative routines. Blade pitch and propeller rpm changes can be carried out manually while calculated thrust and torque can be monitored within Fluent Graphical User Interface (GUI) along with many other parameters used by the VBM algorithm. As

User Defined Memory is allocated for each VBM parameter, those can be accessed during or after the simulations for monitoring or post-processing as required.

As a first step the local flow-field is solved by Fluent and the magnitude of fluid velocity components (v_x, v_y, v_z) are extracted for each cell within the VBM domain. As the VBM domain can be positioned and oriented freely in 3D space, the magnitudes of global velocity components are transformed to the VBM local cylindrical coordinate-system, resulting in axial (v_a), tangential (v_t) and radial (v_r) component magnitudes. This can be done as the positioning and orientation of the VBM domain are known.

The UDF was developed to allow any number of VBM domains to be used within the same Fluent simulation. Each of them can be freely positioned and oriented, the only restriction is that none of the VBM domains can intersect each other or non-fluid regions.

The geometric properties of the propeller and the blades with the operating parameters are defined in a single text file for each VBM domain. These parameters are the followings: speed of rotation (n), number of blades (B), hub and propeller radii (r_{hub}, r_{prop}), blade pitch angle (θ), the distribution of blade chord (C) and twist (γ). Also, the two-dimensional lift (c_l) and drag (c_d) coefficients of dedicated blade sections are stored in input files as a function of radii and local Mach or Reynolds number. c_l and c_d values at specific radii are derived by linear interpolation based on actual blade element radii, Angle of Attack (AoA or α) and Mach number or Reynolds number as specified by the User.

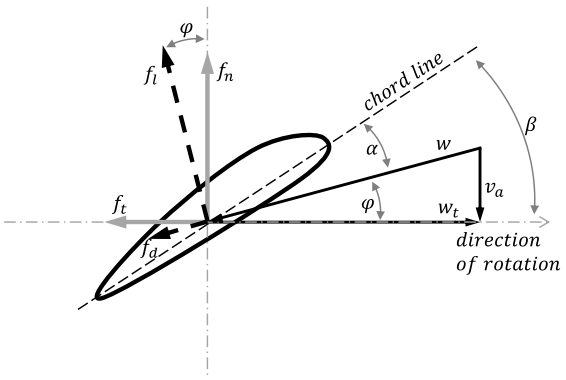

Figure 1. Velocity triangle of a blade element

A typical velocity triangle is depicted in Figure 1. As it is shown in Eqs. (1) to (3) the relative sectional velocity magnitude (w) and its angle relative to the direction of rotation (φ) can be derived from the magnitude of axial and tangential components of the local flow velocity (v_a, v_t,), the propeller speed of rotation (n) and the radii of the actual blade element – which in our case is equal to the distance of the cell centroid (r) measured from the VBM axis.

$$w_t = \omega r + v_t = 2\pi\frac{n}{60}r + v_t \tag{1}$$

$$w = \sqrt{{w_t}^2 + {v_a}^2} \tag{2}$$

$$\varphi = \tan^{-1}\frac{v_a}{w_t} \tag{3}$$

Since the flow-field velocity components are determined from the CFD solution, there is no need to account for any propeller induced velocity components during the calculation process. This induced effect will be implicitly accounted for as the iterative CFD solution progresses.

From the angle φ derived in Eq. (3) and the geometrical properties (θ and γ) the actual AoA (α) for the blade element can be calculated by Eq. (4) following by the calculation of sectional normal and tangential forces for unit span acting on the blade element as given in Eqs. (5) to (6) using the interpolated sectional 2D lift (c_l) and drag (c_d) coefficients. Note, that the effect of radial flow is neglected in the applied model. The compressibility effect or the effect of Reynolds number can be accounted for by using the proper interpolation scheme during the derivation of c_l and c_d.

$$\alpha = \beta - \varphi = \theta + \gamma - \varphi \tag{4}$$

$$f_n = \frac{\rho}{2}w^2 C(c_\mathrm{l}\cos\varphi - c_\mathrm{d}\sin\varphi) \tag{5}$$

$$f_t = \frac{\rho}{2}w^2 C(c_\mathrm{l}\sin\varphi + c_\mathrm{d}\cos\varphi) \tag{6}$$

The calculation described above needs to be carried out for each cell within the VBM domain, using the cell-centroid to determine sectional radii.

Before we can derive the actual source terms for each cell, we need to calculate the magnitudes of the averaged force components induced by the rotating blades at each cell. Based on the work of Wahono [5] we can use the ratio of the mid-cell arc length ($r\,\delta\Psi$) and the distance travelled by the blade element over one revolution ($2\pi r$). Using this arc-length ratio, we can calculate the force magnitudes acting on the fluid volume of a given cell as it is given by Eq. (7) which can be simplified by the expression of cell area in Eq. (8), leading to Eq. (9). This reduction can be utilised for the tangential force component in Eq. (10) as well. Eqs. (9) to (10) were utilised in the VBM UDF.

$$F_n = B \cdot f_n \cdot dr \cdot \frac{r\delta\Psi}{2\pi r} \tag{7}$$

$$A_{cell} = dr \cdot r\,\delta\Psi \tag{8}$$

$$F_n = \frac{B}{2\pi} \cdot f_n \cdot \frac{A_{cell}}{r} \tag{9}$$

$$F_t = \frac{B}{2\pi} \cdot f_t \cdot \frac{A_{cell}}{r} \quad (10)$$

Knowing F_n, F_t and assuming that $F_r = 0$ in the VBM domain cylindrical system allows us to transfer the blade element force components into the absolute cartesian frame of reference ($\underline{F} = [F_x, F_y, F_z]$). As a final step dividing the blade element force vector ($\underline{F}$) by the cell volume (V_{cell}) we can derive the volumetric momentum source term ($\underline{S_U}$) for each cell within the VBM domain, as it is shown in Eq. (11).

$$\underline{S_U} = \frac{1}{V_{cell}} \times \underline{F} \quad (11)$$

2.2. Corrections for Tip-loss

Real flows around rotating propeller blades or rotors are actually complex 3D flows. On the other hand, the implemented 2D-VBM uses 2D profile data. Most of the VBMs, and other analytical methods like Blade Element Momentum theory (BEM) are facing with this problem. Many correction methods have been studied and applied – some with limited, some with greater success [2-6] and [8].

Probably the most common correction method was derived by Prandtl which is assessed in details by Ramdin [8]. Prandtl's method was derived using vortex theory. Fundamentally it is a correction to account for the fact that propellers and rotors have a finite number of blades – correcting the assumption of infinite number of blades applied in ADM and VBM methods. Finite number of finite-span blades forcing the bounding vortex to change rapidly near blade tip, hence reducing lift generation down to zero at the end of the blade [2, 4, 8]. Prandtl derived a correction factor which is the function of the radial position, the blade radii and the distance between two helical wake sheets. The applied 2D-VBM model described in this paper can utilise the Prandtl-Glauert tip loss factor ($F_{Glauert}$) specified in Eq. (12) and the corrected c_l' value from Eq. (13) as it is given in [8].

$$F_{Glauert} = \frac{2}{\pi}\cos^{-1}\left[e^{-\frac{B}{2}\frac{r_{prop}-r}{r_{prop}}\frac{1}{\sin\varphi}}\right] \quad (12)$$

$$c_l' = F_{Glauert}\, c_l \quad (13)$$

In Eq. (13) c_l' is the corrected lift coefficient. We can apply the Prandtl-Glauert correction factor directly to the lift coefficient as there is a linear relationship between the circulation strength and the resultant lift.

3. 3D-VBM

As it can be seen in the previous chapters, all of the ADM, VBM or BEM methods are built on the assumption of infinite number of blades with infinite span, also not accounting for secondary radial flows, however these are clearly non-physical assumptions [8]. Several correction methods exist, like the Prandtl-Glauter tip loss factor which was implemented in our baseline 2D-VBM, but none of these corrections are capable to account for all phenomena which forms the complex 3D flow pattern around rotating blades. Furthermore, most corrections are valid only for a limited geometric and operational parameter range.

The main objective of the consortium working on the KFI-112 tender project was to develop a novel method to account for as many aerodynamic effects as possible regardless of blade geometries or operating conditions.

After the evaluation of fundamentally different concepts, the utilisation of the emerging field of AI was selected as the pillar of the new methodology.

3.1 Process flow

The basic concept is that a trained AI model can predict the behaviour of complex 3D flow phenomena and its effects on the parameters of interest.

In our case it means that using 2D airfoil data – such as c_l and c_d which could be derived from simple inviscid calculations – the AI can predict spanwise force distributions of rotating blades matching explicit 3D CFD results. If the explicit 3D CFD model is validated, we can assume that the AI predicted distributions will closely resemble real case.

The Fluent embedded 3D-VBM process consists of the following five steps:

1. Derivation of local flow parameters (CFD, Fluent)
2. Derivation of AI input dataset (VBM)
3. Derivation of 3D corrected dataset (AI)
4. Derivation of momentum source terms from the 3D corrected dataset (VBM)
5. Update flow field (CFD, Fluent)

The focus was to develop an AI training process required for the 3D-VBM applicable for a given propeller under variable flight conditions – the geometric parameters are kept constant, leaving only the operating parameters to vary. The goal was to make this process applicable for any type of propeller or rotor.

3.2. Generation of the Training Dataset

To train the AI model we need to provide the input dataset and the training dataset which is the desired output for a given input dataset.

The input dataset consists of general operating parameters (flight speed, speed of rotation, blade pitch etc.), propeller performance metrics (overall thrust, torque etc.) and the radial distribution of key parameters (helical Mach number, uncorrected

normal and tangential force etc.). This input dataset is generated by the baseline 2D-VBM using 2D inviscid airfoil data.

The training dataset was the spanwise distributions of normal and tangential forces derived by explicit 3D CFD analyses of the given propeller at different operating conditions. As we considered the explicit 3D CFD results as the reference its validity does not affect the AI training processes and derived corrections, hence it is capable to demonstrate the 3D-VBM method. The discussion of the explicit CFD model is out of the scope of this paper.

3.1. The Artificial Intelligence Model

For the AI model both the input and training data sets were structured into classical tabular (matrix) format.

The input features from the 2D-VBM and the target 3D CFD variables are multidimensional because they are treated as distributions rather than single points. In order to predict a distribution or certain points of a distribution the usage of specific data structures or models are necessary.

Based on practical consideration for the later engineering models, only a sample of points are needed from these distributions as features and as target variables. In the AI models the spanwise distributions were split into discrete points (radial sections). Predictions and the correction model were applied exclusively to these points. The mentioned split means that specific model families should be used which could handle multi response variables, however, these models would be too rigid, because they assume a fixed input/output data structure.

In order to preserve flexibility a work-around was applied combining distribution-like values as section-dependent parameters with other fixed parameters. With this method the correctional model was built successfully as defined in Eq. (14):

$$\xi(x_{i,1}, x_{i,2}, \dots, x_{i,n-1}(s), x_{i,n}(s)) = y_i(s) \tag{14}$$

where, "ξ" represents the AI model, the "$x_{i,n}$" the n-th feature i-th observation, "$x(s)$" and "$y(s)$" are distributional independent and dependent variables, where parameter "s" denotes the section.

Simpler models were tried out first such as linear regression with feature engineering, tree-based methods (e.g., random forest, boosted decision trees), and also explorative analysis and visualisation methods so that we could treat non-linear effects.

The problem could not be modelled precisely and we could not deduct any useful insights with these simpler approaches; presumably because all of the applied variables were of importance in the evaluation of the outcome in such a non-trivial way which these models were not able to unveil adequately.

Finally, the application of a neural network model was decided, which turned out to serve us with trustworthy predictions using a relatively small set of data. Throughout the creation of the neural network, we aspired to create the simplest and smallest architecture to avoid over-fitting.

The final neural network was a simple multi-layer, feedforward network. The hyper-parameter tuning was made using grid-search, the optimised hyper-parameters were the number of neurons, number of layers, activation function, drop-out ratio and other regularisation parameters.

For the activation function a rectified linear unit was used. The most stable and accurate model was a two-layer structure with 200-200 fully-connected dense neurons. By further increase the number of neurons or the number of layers, the model accuracy was not improved and over-fitting became more significant. To overcome the over-fitting phenomenon, several regularisation techniques were tried out, but none of them seemed efficient without decreasing accuracy. By choosing an optimal loss function the model stabilised after all. The Huber loss function as it defined in Eq. (15) was used, known from robust regression models.

$$L = \begin{cases} \frac{1}{2}\|\xi - y\|_2^2 & if \ \|\xi - y\|_1 \leq \delta \\ \|\xi - y\|_1 - \frac{1}{2} & \text{otherwise} \end{cases} \tag{15}$$

For training and testing purposes there were 214 independent observations in total. By varying the distributional section parameters – 20 sections used – we got 4280 partly interdependent observations. The data was split into training and testing parts, based on a unique identifier of the independent observations.

Usage of 60% percent of the data set was sufficient for training, but with larger training size the accuracy and the generalisation capability improved significantly. A test dataset was used only after the training and hyper-parameter optimization phase. During the training and optimization procedure a 4-fold cross-validation technique was applied for monitoring the model stability and performance.

The mean absolute percentage error was 15.45% on average in cross-validation with standard deviation of 0.98 and was 14.2% on the test set.

4. RESULT ASSESSMENT

In the following sections the results derived by the different models will be compared. The reference model is the explicit 3D CFD data which is designated as "Exp.". The baseline 2D-VBM data is designated as "2D" while the tip-loss corrected 2D-

VBM data applying the Prandtl-Glauert correction is designated as "2Dcor". Here the 2D refers to the fact that inviscid 2D airfoil data is used. The data derived using the 3D-VBM model is designated as "3D" referring to the applied AI predicted 3D aerodynamic corrections.

For a better comparison both the Exp. and the VBM model domains were built-up having a constant diameter tube along the rotational axis ranging from the inlet up to the outlet functioning as an infinite constant hub. For each case free-slip wall condition was applied on the surface of this hub.

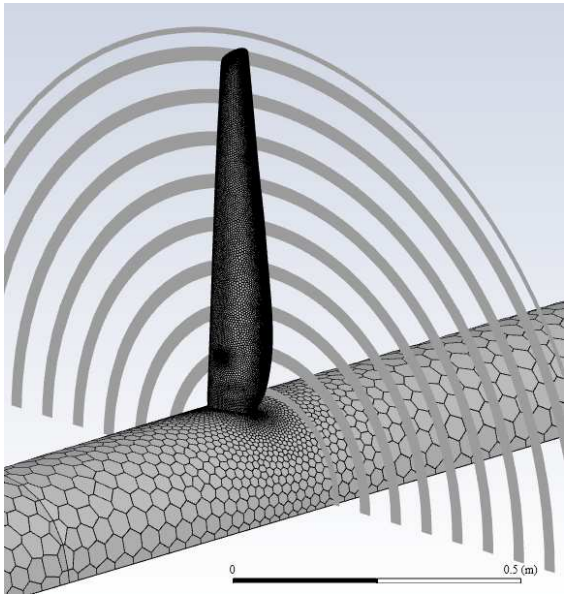

Figure 2. Explicit blade

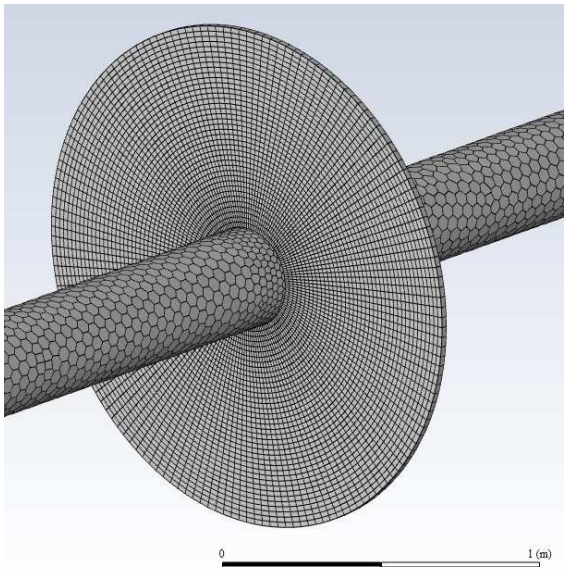

Figure 3. VBM disc

Both the Exp. and VBM CFD domain were built in Fluent Mesher applying poly-hexcore volume mesh with similar volume mesh resolution ensuring better comparability of flow quantities behind the blade and VBM disc. The surface mesh of the explicit blade is depicted in Figure 2 highlighting some of the iso-clip surfaces at 0.1 meter behind the propeller plane used for flow-field evaluation. Figure 3 depicts the structured mesh of the VBM disc and the poly surface mesh of the hub.

The same Fluent solver settings were applied for each model, using the coupled scheme with 2nd order spatial discretization of momentum and pressure, and 1st order upwind for the equations of the applied k-ω SST turbulence model. For the VBM models constant air density was used, while in the explicit 3D CFD model air density was derived using the ideal-gas state equation.

The study was carried out using the CAD model derived by 3D optical scanning technique of an existing propeller blade. The propeller has two blades with a radius of 0.81 meter. The geometric properties and the aerofoil sections were derived from the CAD model. Lift and drag coefficients – which were the basis of all VBM simulations – were derived using XFoil v6.99 (Copyright 2000 Mark Drela and Harold Yougen) assuming inviscid flow, but accounting for the possible variation of local Mach number.

Two different cases are assessed in this paper. The operating conditions for these cases are summarised in Table 1. For each case constant air density were assumed.

Table 1. Operating conditions

Case	*V [m/s]*	*n [rpm]*	*θ [deg]*
Case#1	20	3117	20.0
Case#2	48	2275	39.9

The resulted propeller thrust and torque values for each model are summarized in Table 2 and Table 3 for Case#1 and Case#2, respectively.

Table 2. Case#1 Propeller thrust and torque

Case#1	Thrust [*N*]	Torque [*Nm*]
Exp.	896	98
2D	1189	117
2Dcor.	1068	103
3D	892	96

Table 3. Case#2 Propeller thrust and torque

Case#2	Thrust [*N*]	Torque [*Nm*]
Exp.	1065	275
2D	1753	436
2Dcor.	1188	280
3D	1064	278

As it can be seen from Table 2 and Table 3 both 2D and 2Dcor. show significant deviation from the reference values, while the 3D-VBM propeller thrust and torque agrees very well with the explicit CFD solution. It should be noted that the reference explicit CFD model differs from the one used to generate the AI model training dataset showing the robustness of the 3D correction process.

4.1. Blade load distributions

The spanwise normal force distribution (f_n) was derived from the explicit solutions and compared with the VBM calculated distributions.

It can be concluded from Figure 4 and Figure 5 that the spanwise normal force distributions predicted by the 3D-VBM are in much better agreement with the Exp. results compared to the 2D-VBM and show better agreement than the 2Dcor results, although the 2Dcor. distributions show improved match than the uncorrected 2D-VBM, as it was expected. Similar trends were observed for the tangential force distributions as well.

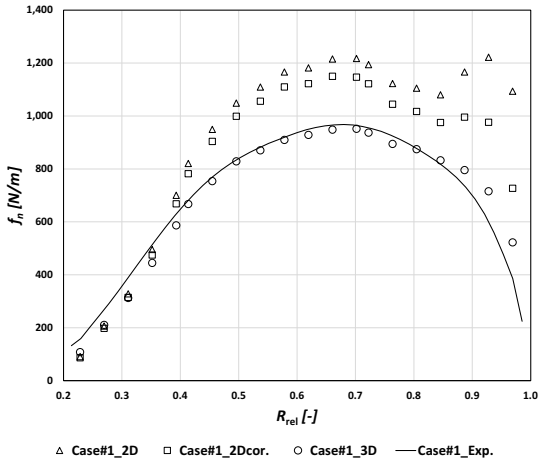

Figure 4. Normal force distributions for Case#1

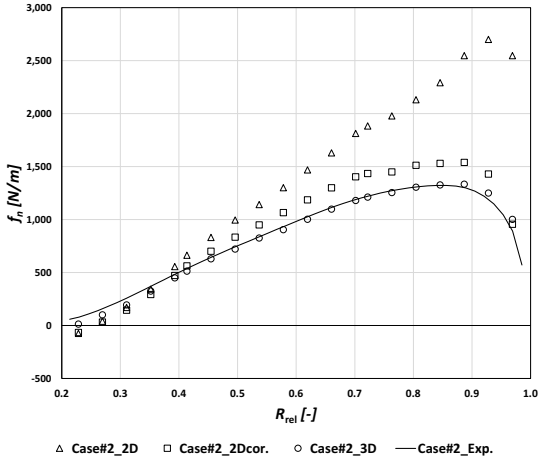

Figure 5. Normal force distributions for Case#2

4.2. Flow-field comparison

An important aspect of comparing different VBM techniques and their accuracy is the flow field assessment downstream the VBM disc and the explicit propeller. Ultimately the purpose of the VBM techniques is the capability to model the propeller induced flow field.

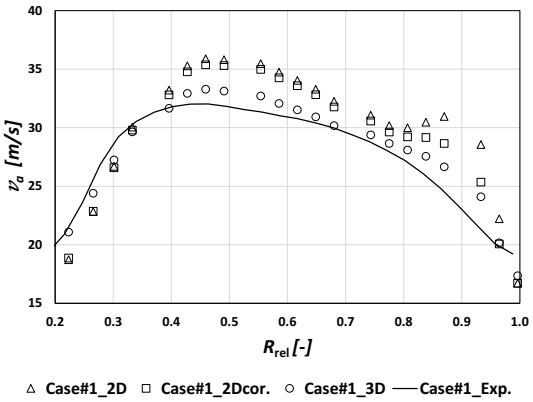

Figure 6. Axial velocity distribution for Case#1

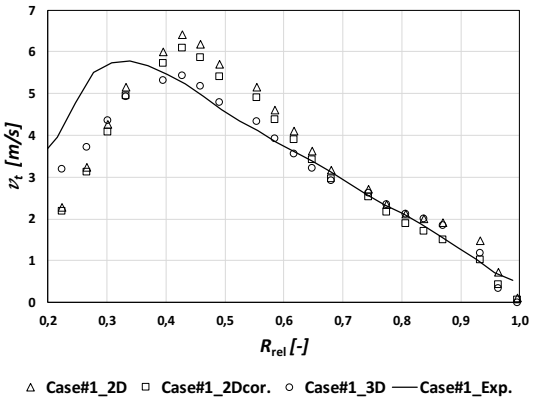

Figure 7. Tangential velocity distribution for Case#1

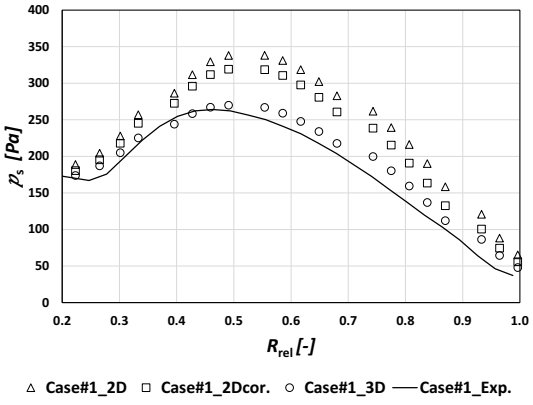

Figure 8. Relative static pressure distribution for Case#1

For this comparison we defined sampling points along a line positioned 0.1 meter behind the VBM disc, where the axial and tangential velocity components and relative static pressure values of the flow were sampled. In order to make it comparable with the VBM results, for the explicit model circumferential surface strips normal to the rotational axis were used, as depicted in Figure 2, to derive the area-averaged values of the investigated parameters. The axial and tangential velocity and relative static pressure distributions are depicted in Figure (6) to (9).

For all depicted distributions the best match with Exp. results were achieved using the 3D-VBM. 2D-VBM shows significant deviations. The 2Dcor. model using the Prandtl-Glauert correction improves the baseline 2D-VBM performance, but still, it is surpassed by the 3D-VBM.

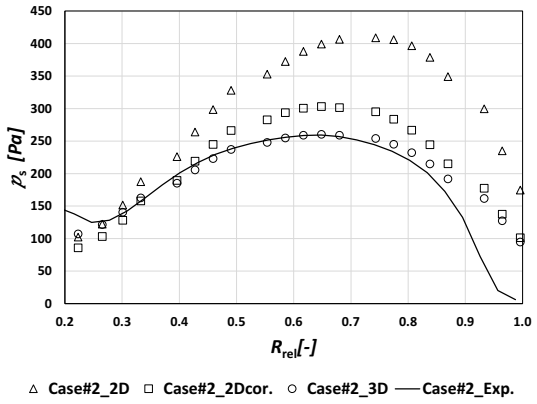

Figure 9. Relative static pressure distribution for Case#2

5. CONCLUSIONS

A new, novel approach for Virtual Blade Model correction was discussed and its superiority over conventional VBM techniques was demonstrated for an existing two bladed general aviation propeller at two operating conditions. It was shown that the propeller performance prediction, spanwise load and flow-field parameter distributions of the explicit CFD model can be matched with improved accuracy by the utilisation of the in-house developed 3D-VBM.

Our aim is to extend the capabilities of the 3D-VBM technique for operating conditions with high rotor inflow angles making the 3D-VBM applicable for the aerodynamic assessment of drones and aircraft with multiple rotors.

ACKNOWLEDGEMENTS

This work has been supported by the Hungarian Government through the NKFI Fund under contract No. 2018-1.2.2-KFI-2018-00057.

REFERENCES

[1] Crouch, Tom D., 2021, "Wright brothers". Encyclopedia Britannica, https://www.britannica.com/biography/Wright-brothers. Accessed 24 January 2022.

[2] Bicsák, Gy, 2017, “Cost Efficient Solutions for Small Aircraft Development Processes Using Numerical Modelling Tools”, *Dissertation Budapest University of Technology and Economics Faculty of Transportation Engineering and Vehicle Engineering Department of Aeronautics, Naval Architecture and Railway Vehicles*, Budapest, Hungary.

[3] Stajuda, M, 2018, “Modified Virtual Blade Method for Propeller Modelling”, *Mechanics and Mechanical Engineering*, Vol. 22, No. 2 (2018) 603-617.

[4] Smith, R. H., 2015, “Engineering Models of Aircraft Propellers at Incidence”, *Dissertation Aerospace Sciences Research Division, School of Engineering, College of Science and Engineering, University of Glasgow,* Glasgow, United Kingdom

[5] Wahono, S., 2013, “Development of Virtual Blade Model for Modelling Helicopter Rotor Downwash in OpenFOAM”, *Aerospace Division, Defence Science and Technology Organisation, Department of Defence, Australian Government,* DSTO-TR-2931

[6] L Wang, Q., Jiang, Z. and Zhang Q., 2014, “Regionalized Actuator Disk Model Designed by Optimisation Method for Propeller Slipstream Computation”, *Engineering Application of Computational Fluid Mechanics*, Vol. 8, pp. 127-139.

[7] Wimshurst, A. and Willden, R., “Validation of an Actuator Line Method for Tidal Turbine Rotors”, Proc. *Department of Engineering Science*, *University of Oxford*, Oxford, United Kingdom.

[8] Ramdin, S. F., 2017, “Prandtl tip loss factor assessed”, *Dissertation Faculty of Aerospace Engineering, Delft University of Technology*, Delft, Netherlands